Islamic University Journal of Applied Sciences (IUJAS)
jesc@iu.edu.sa
Volume VII, Issue I, 1 July 2025, Pages 62-73

Effect of Thermal Configurations in Multi-pipe Heat Exchangers on MHD Natural Convection within a Square Enclosure with Curved Corners

Wedad Hassan Asiri [1], Ammar Abdulkadhim [2], Halemah Ibrahim Elsaeedy [1], Nejla Mahjoub Said [1,*]

[1] Department of Physics, College of Science, King Khalid University, Abha 61413, Saudi Arabia, 445816980@kku.edu.sa; halsayede@kku.edu.sa; nalmahjoub@kku.edu.sa

[2] Mechanical Engineering Department, University of Al-Qadisiyah, Al-Qadisiyah 58001, Iraq, ammar.abdulkadhim@qu.edu.iq

*Corresponding author: (N. Mahjoub), *Email Address*: nalmahjoub@kku.edu.sa

Abstract

This paper aims to study Magnetohydrodynamic (MHD) natural convection in a square enclosure with curved corners, particularly the thermal performance of multi-inner pipes used in heat exchangers. Numerical simulations are carried out to study the fluid flow behavior and thermal distribution in the presence of magnetic field by changing Hartmann number from [0-80] and varying Rayleigh number [1e4-1e6]. It can be seen that the layout of the inner pipes has a great influence on the enhancement of heat transfer rates and some recommendations for the improvement of the heat exchange design for engineering applications are provided. Finally, conclusions are made based on the numerical results of this study. The results showed that increasing Ra and reduced Ha reveals better heat transfer. Additionally, at high, case 1 give the best heat transfer bettering.

Keywords: Magnetohydrodynamics (MHD), Heat Transfer Enhancement, Nusselt Number (Nu), Nanofluid Thermodynamics, Numerical Simulations

https://doi.org/10.63070/jesc.2025.005
Received 02 April 2025; Revised 06 May 2025; Accepted 18 May 2025.
Available online 25 May 2025.

1. Introduction

There are thousands of published articles on natural convection within enclosures due to its applications in the heat exchangers industry. Generally, this field can be categorized into two major groups: (1) studies without an inner body and (2) studies with an inner body. The first category has been extensively examined by numerous researchers considering various thermal arrangements. Alasiri (2024) numerically investigated the effects of heater length and position on natural convection in a square enclosure filled with Cu-water nanofluid. A correlation for the Nusselt number was developed in terms of heater parameters, Rayleigh number, and nanoparticle loading.

Ghasemi and Aminossadati (2009) numerically analyzed the impact of inclination angle on heat transfer properties within a square enclosure filled with CuO-water nanofluid. For this purpose, the finite volume method was used in the numerical solution. Their results showed that the inclination angle plays a significant role in determining the heat transfer rate. The second category, which focuses on the role of the inner body, has also been widely studied.

For example, Kim et al. (2008) investigated the effects of the vertical position of an inner circular body located within a square enclosure under different Rayleigh numbers. The Immersed Boundary Method (IBM) was employed in the numerical simulations. Their findings indicated that the highest Nusselt number along the inner body occurs when it moves downward. Other studies have explored configurations with multiple inner bodies.

Garoosi et al. (2015) examined natural convection within a square enclosure containing multiple hot and cold inner bodies. The authors analyzed various types of nanofluids, including Cu, Al_2O_3, and TiO_2, along with different numbers and locations of inner bodies. Their results demonstrated that the placement of inner bodies significantly influences the heat transfer rate. Additionally, the role of the magnetic field was investigated to assess its impact on fluid flow and heat transfer characteristics.

Cho et al. (2019) conducted a numerical study on two-dimensional natural convection in a square container featuring a vertical array of two elliptical cylinders. They employed the Immersed Boundary Method (IBM) combined with the Finite Volume Method (FVM) to accurately capture the virtual wall boundaries of the cylinders. The aspect ratio (AR) of the elliptical cylinders varied from 0.25 to 4.00, while the Rayleigh number (Ra) ranged from 10^4 to 10^6. The study analyzed changes in flow and thermal fields resulting from different aspect ratios of the elliptical cylinders.

Ibrahim et al. (2022) investigated natural convection inside cavities to enhance heat transfer in different package shapes by introducing nanoparticles into the core fluid. They used the COMSOL software, based on the Galerkin finite element approach, for their numerical calculations. The study considered

various parameters, including Rayleigh numbers (10^3 to 10^6), solid volume fraction (Ø=0.05), inclination angles (-45°, -30°, 0°, 30°, 45°), the radius of the inner circle (R=0.15), and the radii of the inner elliptical cylinder (R_x=0.2 and R_y=0.15).

Nammi et al. (2022) numerically investigated unsteady natural convection heat transfer in a porous square container containing four heated cylinders arranged in either a square or rectangular configuration. The results were presented using streamlines, isotherms, and time-averaged Nusselt numbers for the ranges $10^3 \leq$ Ra $\leq 10^6$, $10^{-4} \leq$ Da $\leq 10^{-2}$, and four different cylinder spacings ($0.3 \leq S \leq 0.6$).

Chatterjee and Kumar (2017) conducted a finite-volume numerical study on two-dimensional hydromagnetic natural convection in a cooled square container containing four uniformly shaped, heated inner circular cylinders. They assumed that all solid walls were electrically insulated. The simulations covered various control parameters, including Rayleigh numbers (10^3 to 10^6), Hartmann numbers (0 to 50), and dimensionless distances between cylinder centers (0.3 to 0.7). The study aimed to analyze how the placement of the cylinders along the diagonals of the enclosure influences magnetic heat transfer within the cavity.

The present work focuses on natural convection heat transfer within a square enclosure with curved corners, filled with different thermal arrangements of inner bodies, using the finite element method under a horizontal magnetic field. Numerical simulations were conducted to analyze the effects of various thermal arrangements and configurations of inner pipes on heat transfer performance. Using COMSOL Multiphysics, the fluid flow behavior and thermal distribution were studied under the influence of a magnetic field and varying Rayleigh numbers. The governing mathematical equations for fluid flow, heat transfer, and magnetic field interactions were solved to ensure accurate and reliable results. The findings demonstrated that the layout and configuration of the inner pipes significantly influence heat transfer rates, providing valuable insights into optimizing heat exchanger design for engineering applications. Based on the numerical results, recommendations were provided for improving thermal performance. Future studies could explore more complex geometries and turbulent flow conditions to further enhance the understanding of heat transfer mechanisms in magnetohydrodynamic (MHD) systems.

2. Material and method

The computation domain considering four different cases of inner hot and cold bodies presented in Figure 1. The governing equations had been inserted below;

$$\frac{\partial U}{\partial X}+\frac{\partial V}{\partial y}=0$$

$$U\frac{\partial U}{\partial X}+V\frac{\partial U}{\partial Y}-\frac{\partial P}{\partial x}+\frac{\mu_{nf}}{\rho_{nf}\alpha_f}\left(\frac{\partial^2 U}{\partial^2 X}+\frac{\partial^2 U}{\partial^2 Y}\right)$$

$$U\frac{\partial V}{\partial X}+V\frac{\partial V}{\partial Y}=-\frac{\partial P}{\partial Y}+\frac{\mu_{nf}}{\rho_{nf}\alpha_f}\left(\frac{\partial^2 V}{\partial^2 X}+\frac{\partial^2 V}{\partial^2 Y}\right)-Ha^2\cdot PrV+Ra\cdot\frac{\Pr(\rho\beta)_{nf}}{\rho_{nf}\beta_f}\theta$$

$$U\frac{\partial \theta}{\partial X}+V\frac{\partial \theta}{\partial Y}=\frac{\alpha_{n_f}}{\alpha_f}\left(\frac{\partial^2 \theta}{\partial X^2}+\frac{\partial^2 \theta}{\partial Y^2}\right)$$

The following nondimensional parameters had been considered;

$$X=\frac{X}{L},Y=\frac{y}{L},A=\frac{a}{L},B=\frac{b}{L},U=\frac{uL}{\alpha_f},V=\frac{vL}{\alpha_f},P=\frac{\bar{P}L^2}{\rho_{nf}\alpha_f^2},\theta=\frac{T-T_c}{T_h-T_c}$$

Three dimensionless numbers had been involved in the present study;

$$Ra=\frac{g\beta_f L^2(T_h-T_c)}{v_f\alpha_f},Ha=B_0L\sqrt{\frac{\sigma_{nf}}{\rho_{nf}v_f}},\ Pr=\frac{v_f}{\alpha_f},Nu_m=\frac{1}{S}\int_0^S Nu\,(S)ds$$

where S is the surface area of the inner body

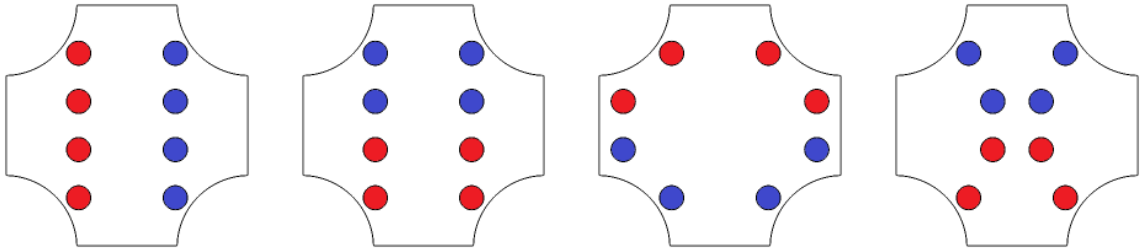

Case 1 Case 2 Case 3 Case 4

Figure 1. schematic representation of the problem

The properties of the nanofluid can be defined based on the properties of the pure liquid and solid nanoparticles (Oztop and Nada 2008)

$$\rho_{nf}=(1-\phi)\rho_f+\phi\rho_s\,,(\rho\beta)_{n_f}=(1-\phi)(\rho\beta)_f+\phi(\rho\beta)_s$$

$$\left(\rho C_p\right)_{nf}=(1-\phi)\left(\rho C_p\right)_f+\phi\left(\rho C_p\right)_5,\alpha_{nf}=\frac{k_{nf}}{(\rho C_p)_{nf}},\sigma_{nf}=(1-\phi)\sigma_f+\phi\sigma_s$$

$$k_{nf}=\frac{(k_P+2k_f)-2\phi(k_f-k_p)}{(k_f+2kp)+\phi(k_f+k_p)}k_f;\mu_{nf}=\mu_f(1-\phi)^{-2.5}$$

Table 1. the thermophysical properties of the base fluid and CuO (Ghasemi and Aminossadati 2010)

	Pure water	CuO
$\boldsymbol{\rho}$ (kgm^{-3})	997.1	6320
$C_p(Jkg^{-1}K^{-1})$	4179	531.8
K (W$m^{-1}k^{-1}$)	0.613	76.5
$\beta \times 10^{+5}(k^{-1})$	21	1.8

2.1 Mesh generation

COMSOL software was used to draw the model, generate the grid as presented in Figure 2, and then solve the governing equations using the finite element method.

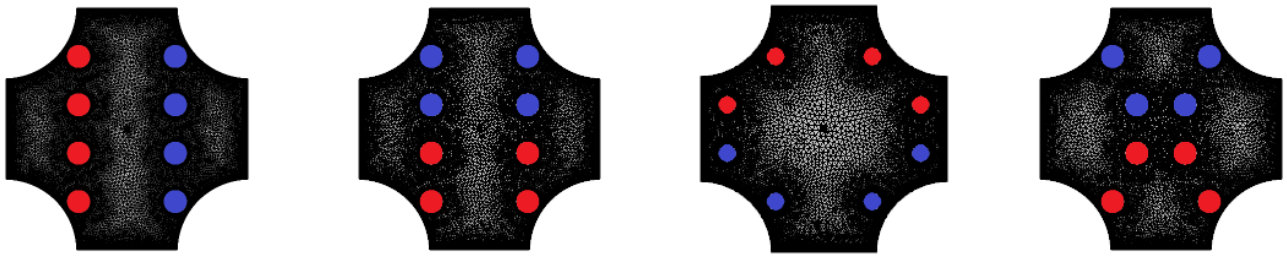

Case 1 Case 2 Case 3 Case 4

Figure 2. mesh generation for the four cases

2.2 Validation

The validation had been done with Davis (1983) in terms of Nusselt number as depicted in Figure 3 under various Rayleigh numbers.

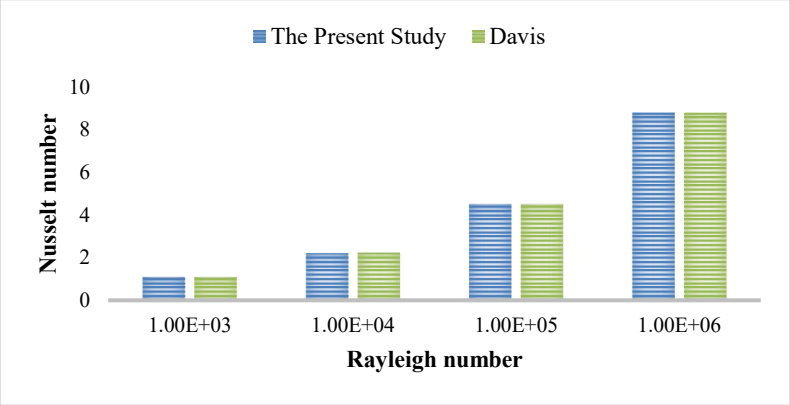

Figure 3. validation of the present work with Davis (1983)

3. Results and discussions

Figure 4.a. illustrates the streamlines and isothermal contours for different Hartmann numbers (Ha) at a constant Rayleigh number Ra=10^4 for case 1. The streamlines represent the flow behavior and circulation patterns within the domain, highlighting the magnetic field's influence on natural convection. At Ha=0, the flow exhibits strong vortex patterns with prominent buoyancy effects. As Ha increases (Ha=40 and Ha=80), the flow patterns become more organized due to the Lorentz force induced by the magnetic field, reducing circulation and minimizing flow disturbances. The isothermal contours illustrate the temperature distribution within the domain. At Ha=0, the contours are irregular and widely spaced, indicating convection-dominated heat transfer. As Ha increases, the isothermal contours become more uniform and closely spaced, reflecting the reduced impact of convection as the magnetic field enhances conduction. The combined effect of the magnetic field and higher Hartmann numbers reduces flow disturbances and promotes heat transfer through conduction, resulting in a more stable thermal distribution across the domain.

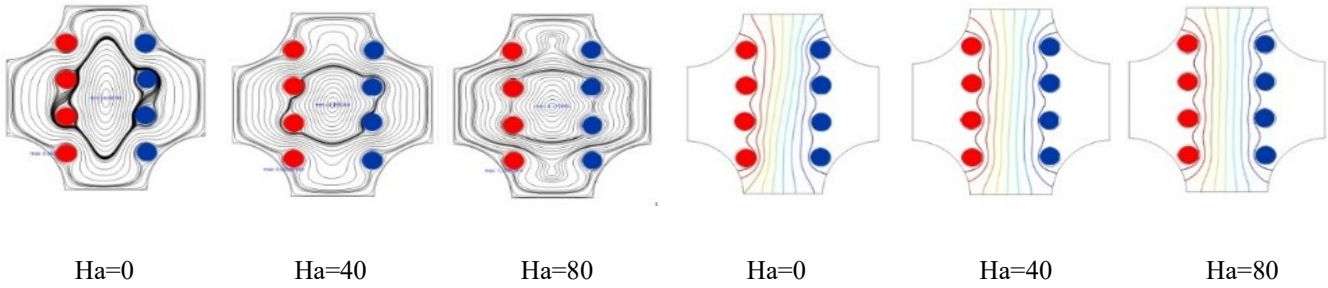

Ha=0 Ha=40 Ha=80 Ha=0 Ha=40 Ha=80

a. Ra=10^4

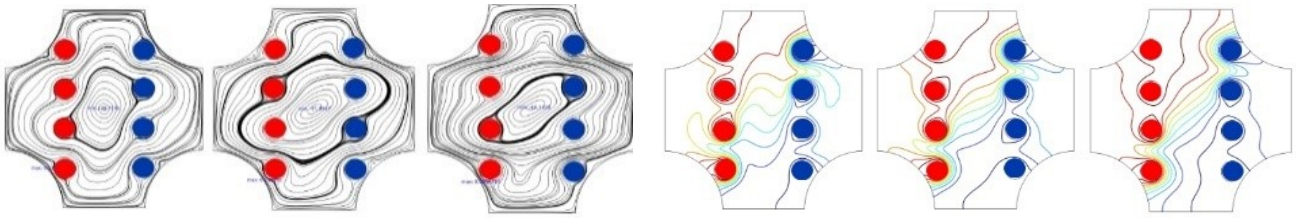

Ha=0 Ha=40 Ha=80 Ha=0 Ha=40 Ha=80

b. Ra=10^6

Figure 4. Streamlines and isotherms for various Hartmann numbers: case 1

Figure 4.b illustrates the streamlines and isothermal contours for different Hartmann numbers (Ha=0, 40, 80) at a constant Rayleigh number (Ra=10^6) for case 1. The streamlines depict variations in flow

behavior and circulation patterns within the domain, highlighting the influence of the magnetic field at different Hartmann numbers.

At Ha=0, the flow exhibits strong vortex structures due to the dominant buoyancy effect. As Ha increases, the flow patterns become more structured, demonstrating the magnetic field's role in suppressing natural convection and reducing flow disturbances. The isothermal contours represent the temperature distribution within the domain. At Ha=0, the contours appear distorted and irregular, indicating convection-dominated heat transfer. As Ha increases, the isothermal contours become more uniform, reflecting a transition toward conduction-dominated heat transfer under the influence of the magnetic field. The combined effect of the magnetic field and higher Hartmann numbers enhances thermal conduction while suppressing convection, leading to a more stable and uniform temperature distribution within the domain.

Figure 5.a illustrates the streamlines and isotherms for various Hartmann numbers (Ha=0, 40, 80) at a constant Rayleigh number (Ra=10^4) for case 2.

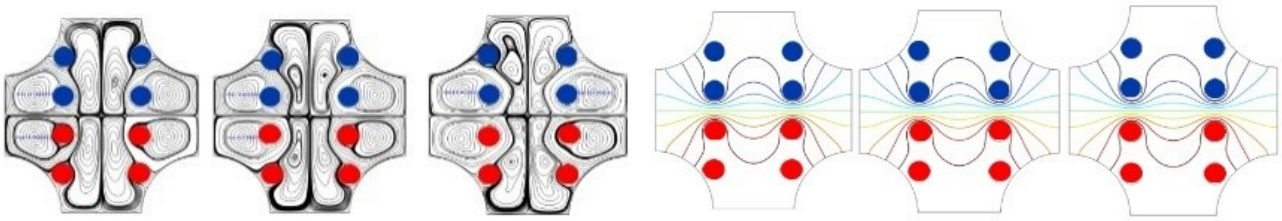

Ha=0 Ha=40 Ha=80 Ha=0 Ha=40 Ha=80

a. Ra=10^4

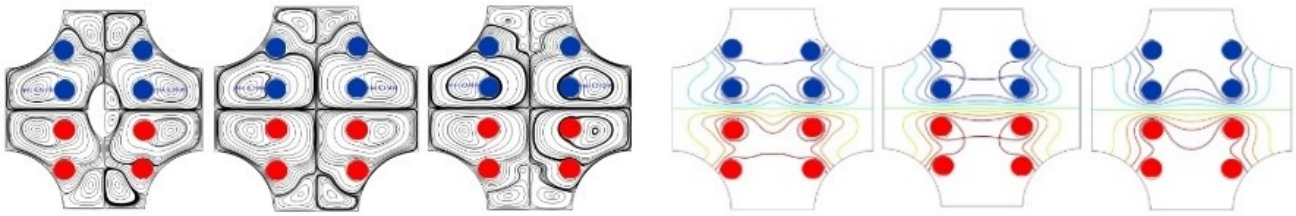

Ha=0 Ha=40 Ha=80 Ha=0 Ha=40 Ha=80

b. Ra=10^6

Figure 5. Streamlines and isotherms for various Hartmann numbers: case 2

The streamlines depict fluid flow behavior within the domain and the influence of the magnetic field on circulation patterns. At Ha=0, the flow exhibits strong vortical structures driven by natural convection. As Ha increases, the streamlines become more organized, reflecting the dampening effect of the magnetic field, which reduces flow disturbances and suppresses convective motion. The isotherms represent the temperature distribution within the domain. At Ha=0, they appear distorted and irregular, indicating convection - dominated heat transfer. As Ha increases, the isotherms become smoother and more uniform, signifying a transition to conduction-dominated heat transfer. This figure highlights the increasing influence of the magnetic field in suppressing convection and enhancing thermal conduction, leading to a more stable and uniform temperature distribution.

Figure 5.b. illustrates the streamlines and isotherms for various Hartmann numbers (Ha=0,40,80) at a constant Rayleigh number (Ra=10^6) for case 2. The streamlines depict the dynamic behavior of the flow and circulation patterns within the domain. At Ha=0, the flow exhibits strong vortices driven by natural convection in the absence of a magnetic field. As Ha increases to 40 and 80, the vortex intensity gradually decreases, with the flow becoming more stable and less dynamic due to the suppressive effect of the magnetic field on convection, with reduces flow velocity. The progressive change in flow patterns demonstrates how the magnetic field stabilizes the flow and mitigates disturbances caused by natural convection. The isotherms represent the temperature distribution within the domain. At Ha=0, the isotherms are highly distorted, indicating convection-dominated heat transfer. As Ha increases to 40 and 80, the isotherms become more uniform and parallel, signifying a transition to conduction-dominated heat transfer and a diminished influence of convection. This figure highlights the combined effects of the magnetic field and constant Rayleigh number, where the magnetic field enhances system stability, suppresses convective effects, and promotes heat transfer through conduction.

Figure 6.b. illustrates the streamlines and isotherms for various Hartmann numbers (Ha=0, 40, 80) at a constant Rayleigh number (Ra=10^6) for case 3. The streamlines depict the flow patterns within the domain. showing strong vortices at Ha=0, which indicate the dominance of natural convection in the absence of a magnetic field. As Ha increases to 40 and 80, the intensity of the vortices gradually diminishes, reflecting the suppressive effect of the magnetic field on convective motion and its role in stabilizing the flow. The magnetic field reduces the kinetic energy of convection and enhances the steadiness of the flow. The isotherms represent the heat distribution within the domain. At Ha=0, the isotherms are highly distorted due to intense heat transfer driven by strong convection. As Ha increases, the isotherms become more uniform and parallel, indicating the dominance of conduction over convection. This figure highlights the influence of the magnetic field in mitigating convection

and promoting conduction-based heat transfer, resulting in a more stable and efficient heat distribution system.

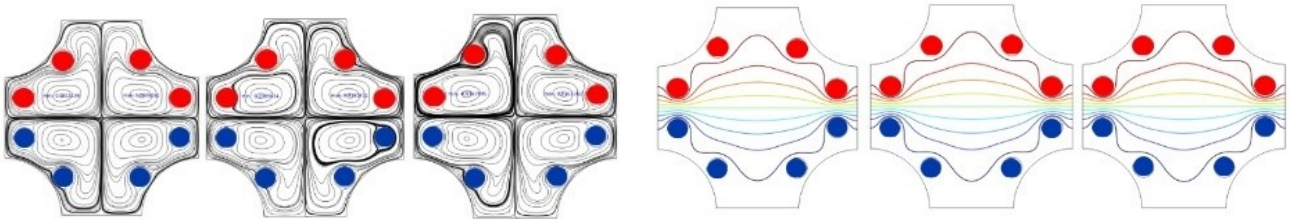

Ha=0 Ha=40 Ha=80 Ha=0 Ha=40 Ha=80

Figure 6. Streamlines and isotherms for various Hartmann numbers: case 3 at Ra = 10^6

Figure 7.a. illustrates the streamlines and isotherms for various Hartmann numbers Ha at a constant Rayleigh number Ra = 10^4 for case 4. In the top row, the streamlines depict the fluid flow patterns within the domain. At Ha = 0, the flow motion is prominent with strong vortices, reflecting the effects of unconstrained natural convection. As Ha increases to 40 and 80, the intensity of the vortices gradually decreases, indicating that the magnetic field restricts the flow motion and weakens the buoyancy effects. In the bottom row, the isotherms show the temperature distribution within the domain. At Ha = 0, the isotherms are highly distorted due to heat transfer dominated by convection. As Ha increases, the isotherms become more regular and align closer to the conductive pattern, highlighting the effect of the magnetic field in reducing convection intensity and enhancing conductive heat transfer. The figure emphasizes the interaction between buoyancy forces and the magnetic field, where the magnetic field suppresses thermal flow and modifies the heat distribution pattern

Figure 7.b. illustrates the streamlines and isotherms for various Hartmann numbers Ha at a constant Rayleigh number Ra=10^6 for case 4. The streamlines in the top section represent the flow behavior and circulation patterns within the domain, highlighting the influence of the magnetic field as Ha increases. At Ha = 0, the flow exhibits strong circulation patterns and well-defined vortices, reflecting the intense natural convection effects driven by buoyancy forces. As Ha increases to 40 and 80, the streamlines show a gradual reduction in circulation intensity, indicating that the magnetic field suppresses motion and diminishes the effects of convection. The isotherms in the bottom section depict the temperature distribution across the domain. At Ha = 0, the isotherms are highly distorted, indicating heat transfer dominated by convection. As Ha increases to 40 and 80, the isotherms become more regular and parallel, reflecting a transition to conduction-dominated heat transfer due to the influence

of the magnetic field. The figure demonstrates how the magnetic field reduces the intensity of convection and enhances conduction, contributing to a more stable and uniform heat distribution within the domain.

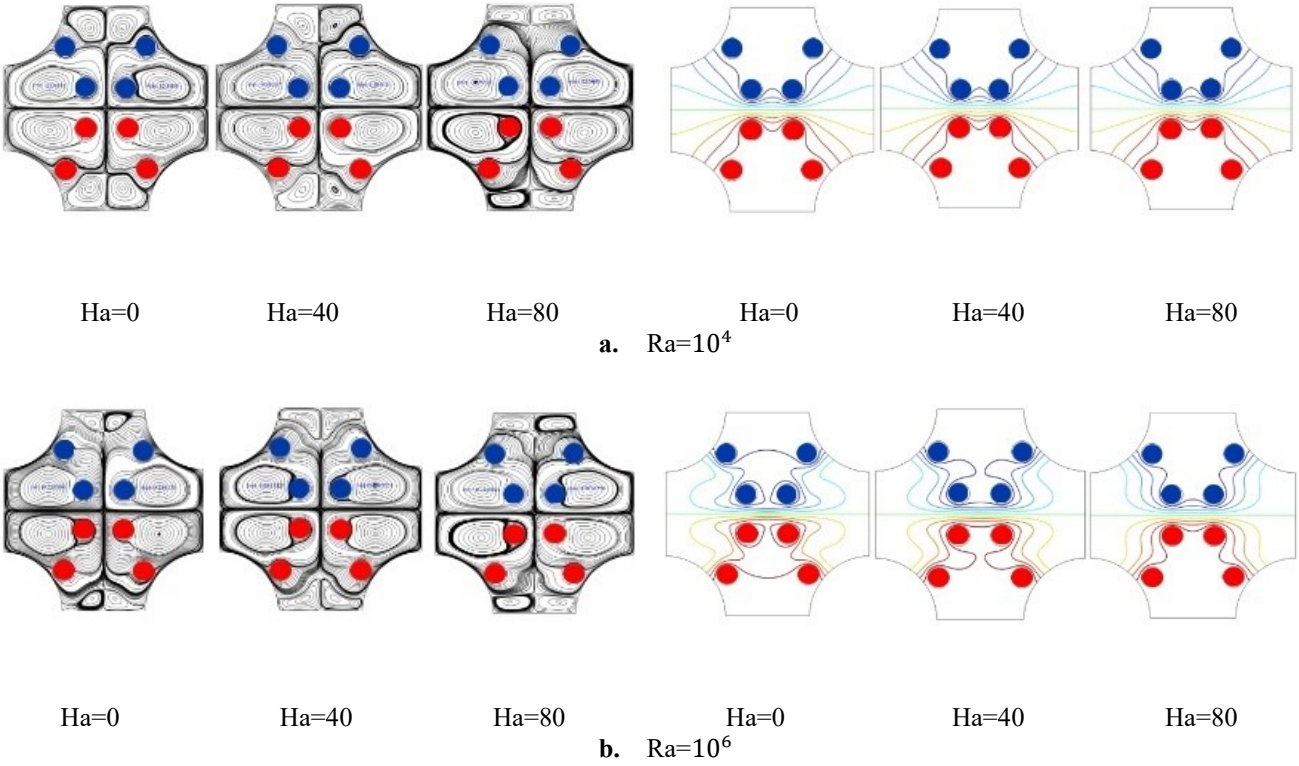

Figure 7. Streamlines and isotherms for various Hartmann numbers: case 4

Figure 8a illustrates the variation of the average Nusselt number (Nu) at a fixed Rayleigh number (Ra= 10^4) as the Hartmann number (Ha) increases. The graph shows that Nu remains constant, indicating that the magnetic field has an insignificant effect on heat transfer in this case. All the studied cases exhibit stable and similar behavior, suggesting that natural convection is relatively weak at this Rayleigh number. Consequently, the Lorentz force induced by the magnetic field is insufficient to significantly alter the thermal distribution. These findings suggest that at a low Ra, the magnetic field does not notably impact heat transfer through natural convection. Figure 8b illustrates the variation of the average Nusselt number (Nu) at a fixed Rayleigh number (Ra= 10^6) as the Hartmann number (Ha) increases. The graph shows a significant decrease in Nu, indicating that the magnetic field has a clear suppressive effect on heat transfer via natural convection at higher Ha values. The decline in Nu is more pronounced in the first case compared to the others, suggesting that the geometric configuration or nanofluid distribution influences the system's response to the magnetic field. The gradual decrease in heat transfer efficiency further indicates that the Lorentz force opposes the natural thermal flow,

limiting convective heat transfer. These findings suggest that the impact of the magnetic field becomes more pronounced as the Rayleigh number increases.

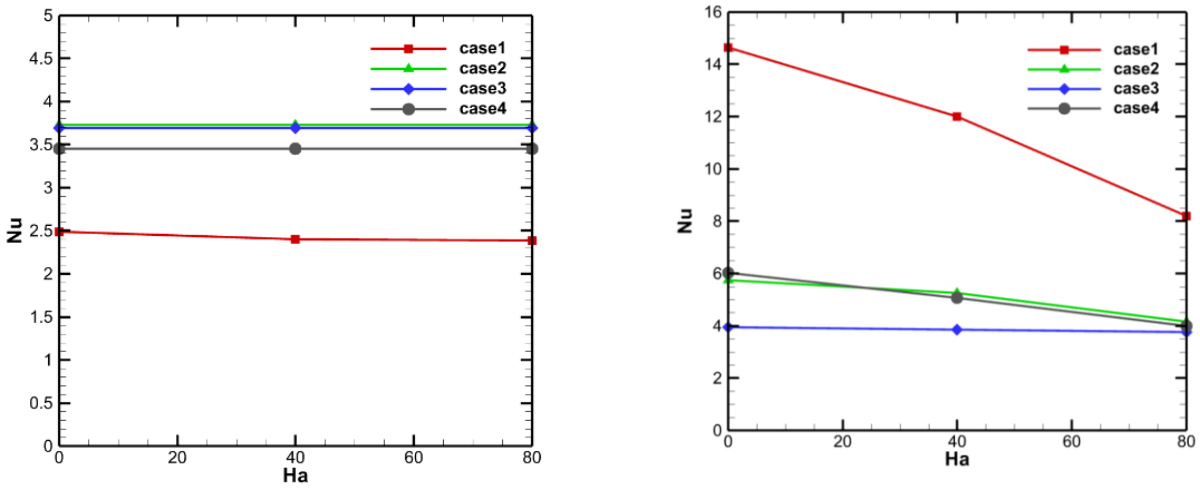

$a. 10^4$ $b.\ 10^6$

Figure 8. Nusselt number with Hartmann number considering four different cases

4. Conclusion

This study investigated Magnetohydrodynamic (MHD) natural convection in a square enclosure with curved corners, focusing on the thermal performance of multi-inner pipes used in heat exchangers. The key findings are summarized as follows:

1. At low Rayleigh number (Ra), case 1 recorded the lowest average Nusselt number (Nu).
2. In contrast, case 1 also exhibited the highest Nu under different conditions.
3. The impact of the Hartmann number (Ha) is significant for case 1, while it is negligible for case 3

Reference

[1] Alasiri, A. (2024) The Role of Heater Size and Location in Modulating Natural Convection Behavior in Cu-Water Nanofluid-Loaded Square Enclosures. Sustainability, 16(22): p. 9648.
[2] Chatterjee, D. and S. Kumar Gupta (2017) Magnetohydrodynamic natural convection in a square enclosure with four circular cylinders positioned at different rectangular locations. Heat Transfer Engineering, 38(17): 1449-1465.
[3] Cho, H.W., M.Y. Ha, and Y.G. Park (2019) Natural convection in a square enclosure with two hot inner cylinders, Part II: The effect of two elliptical cylinders with various aspect ratios in a vertical array. International Journal of Heat and Mass Transfer, 135: 962-973.
[4] Davis Vahl, G. (1983) Natural convection of air in a square cavity: a bench mark numerical solution. International Journal for numerical methods in fluids, 3(3): 249-264.

[5] Garoosi, F., et al. (2015) Numerical simulation of natural convection of the nanofluid in heat exchangers using a Buongiorno model. Applied Mathematics and Computation, 254: 183-203.
[6] Ghasemi, B. and S. Aminossadati (2009) Natural convection heat transfer in an inclined enclosure filled with a water-CuO nanofluid. Numerical Heat Transfer, Part A: Applications, 55(8): 807-823.
[7] Ghasemi, B. and S. Aminossadati (2010) Brownian motion of nanoparticles in a triangular enclosure with natural convection. International Journal of Thermal Sciences, 49(6): 931-940.
[8] Ibrahim, M.N.J., et al. (2022) Study of natural convection inside inclined nanofluid cavity with hot inner bodies (circular and ellipse cylinders). International Journal of Heat and Technology, 40(3): 699-705.
[9] Kim, B.S., et al. (2008) A numerical study of natural convection in a square enclosure with a circular cylinder at different vertical locations. International Journal of Heat and Mass Transfer, 51(7): 1888-1906.
[10] Nammi, G., et al. (2022) Natural convection heat transfer within a square porous enclosure with four heated cylinders. Case Studies in Thermal Engineering, 30: 101733.
[11] Oztop, H.F. and E. Abu-Nada (2008) Numerical study of natural convection in partially heated rectangular enclosures filled with nanofluids. International Journal of Heat and Fluid Flow, 29(5): 1326-1336.